Minimal mechanism leading to discontinuous phase transitions for short-range systems with absorbing states

Carlos E. Fiore
Instituto de Física, Universidade de São Paulo Caixa Postal 66318, 05315-970 São Paulo, Brazil
(Received 17 July 2013; revised manuscript received 5 November 2013; published 6 February 2014)

Motivated by recent findings, we discuss the existence of a direct and robust mechanism providing discontinuous absorbing transitions in short-range systems with single species, with no extra symmetries or conservation laws. We consider variants of the contact process, in which at least two adjacent particles (instead of one, as commonly assumed) are required to create a new species. Many interaction rules are analyzed, including distinct cluster annihilations and a modified version of the original pair contact process. Through detailed time-dependent numerical simulations, we find that for our modified models, the phase transitions are of first order, hence contrasting with their corresponding usual formulations in the literature, which are of second order. By calculating the order-parameter distributions, the obtained bimodal shapes as well as the finite-scale analysis reinforce coexisting phases and thus a discontinuous transition. These findings strongly suggest that the above particle creation requirements constitute a minimum and fundamental mechanism determining the phase coexistence in short-range contact processes.

DOI: 10.1103/PhysRevE.89.022104 PACS number(s): 05.70.Ln, 05.50.+q, 05.65.+b

I. INTRODUCTION

Nonequilibrium phase transitions into absorbing states have attracted great interest in recent years, not only for the possibility of describing a countless number of processes, such as wetting phenomena, spreading of diseases, and chemical reactions [1,2], but also for the search for experimental realizations [3]. In the simplest examples, they manifest in single-species systems, such as probabilistic cellular automata or contact processes (CPs) [1,4]. Typically, these transitions are second order, belonging to the directed percolation (DP) universality class [2]. Although infrequent in the above situations, discontinuous absorbing transitions have also been observed. Mean-field approaches [5], lattice models [6–8], and continuous descriptions [9] reveal that their occurrence requires an effective mechanism that suppresses low-density states. According to the Elgart-Kamenev classification [10], for one-component reaction diffusion with n-particle creation and k-particle annihilation, the reactions $kA \to (k-l)A$ and $nA \to (n+m)A$ summarize the existence of a discontinuous transition whenever $k < n$. Although such semiclassical field theory is an important benchmark, suggesting crucial ingredients for its occurrence, the system dimensionality or the inclusion of spatial fluctuations may suppress the stabilization of compact clusters in the above conditions [11,12].

Inspired by mean-field-like predictions [5], some *restrictive* versions of the two- and three-dimensional CPs [4] have been considered [13–15]. They differ from the original case in which more than one nearest-neighbor occupied site is required to create a new particle (instead of one as in the standard CP) and single particles are annihilated. In the simplest case [15], two particles are required and the creation does not depend on the specific particle displacements, as exemplified in Fig. 1(a). Unlike the original CP, the transition becomes discontinuous for dimensions larger than 1. Extension of such interactions for complex networks [16] (instead of regular lattices [13–15]) has revealed that the topology of the lattice does not affect the phase coexistence. In contrast, by changing the dynamics mildly, where one nearest-neighbor pair is necessary to create a new offspring (instead of two nearest-neighbor particles but still fulfilling the condition $k < n$) the phase coexistence is suppressed, becoming continuous again (schematically, such a change is equivalent to shifting the local rule of particle creation at 0 from 1-0-1 to 1-1-0). All these comments inspire us to raise two fundamental questions: Is there an ingredient that always provides a discontinuous absorbing transition in single-species systems? If so, what is this dynamics? To try to answer such questions, we investigate thoroughly a class of four restrictive processes. In the first three examples, we consider the particle creation in the presence of at least two particles (as considered in Ref. [15]) and a family of annihilation processes (to be described further). Our goal is to verify if the phase coexistence is maintained by changing the annihilation rules. The fourth model is a small modification in the pair contact process (PCP), a notorious model with infinitely many absorbing states and a DP phase transition [17,18]. In our modified version, at least two pairs of particles are required (instead of one as in the original PCP) to create a new particle. This modification aims to verify if, similarly to previous cases, this small change is sufficient to shift the order of transition. As will be shown, under two distinct methodologies, in all restrictive models the phase transition is first order, which suggests that the particle creation in the presence of a minimal neighborhood (for the studied models it is 2) constitutes a fundamental (and robust) mechanism ruling discontinuous absorbing phase transitions.

II. MODELS AND METHODS

In all the situations considered here, if a site i is empty (occupied) then the occupation variable η_i assumes the value 0 (1). In the first three model versions, when $\eta_i = 0$ a particle can be created at i with a probability $\mathcal{N}/z$ for $\mathcal{N} \geqslant 2$ and zero otherwise [Fig. 1(a)]. There is no creation if $\mathcal{N} \leqslant 1$. Here $\mathcal{N}$ is the number of occupied neighbors of i and z is the lattice coordination number. In a square lattice (all our studies)

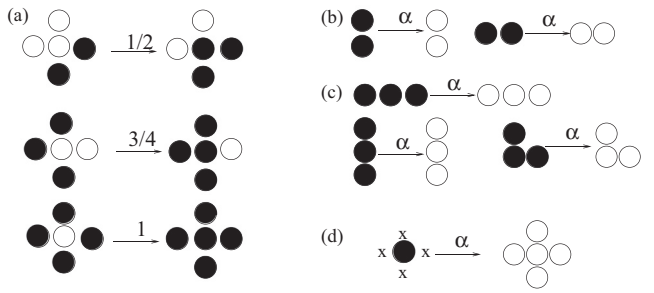

FIG. 1. Examples of transition rates in a square lattice ($z = 4$). Models A, B, and C are defined by the (a)-(b), (a)-(c), and (a)-(d) interaction rules, respectively. In (d), the symbol $\times$ denotes a local configuration composed of $\mathcal{N}$ nearest-neighbor occupied sites (with $\mathcal{N}$ ranging from 0 to 4) and after the annihilation all $\mathcal{N}+1$ particles are extinct.

$z = 4$. In a similar fashion, particles can be annihilated with a probability α (according to the rules described below).

In model A, annihilation occurs only for pairs of adjacent particles ($k = l = 2$). Thus, an isolated particle cannot be destroyed [Fig. 1(b)]. For model B, annihilation occurs only for three adjacent particles ($k = l = 3$) [Fig. 1(c)]. Thus, neither isolated particles nor pairs of particles are eliminated. Finally, in model C the annihilation of a particle at site i automatically wipes out all its $\mathcal{N}$ nearest-neighbor occupied sites ($k = l = \mathcal{N}+1$) [Fig. 1(d)]. Therefore, contrasting with A and B, the number of exterminated particles is not fixed, ranging from 1 to 5 in a square lattice (recall that $\mathcal{N}$ varies from 0 to 4 in a square lattice). Thus, for models B and C, the Elgart-Kamenev classification is violated. The last one, model D, is a modification of the PCP [17,18]. In the original PCP, only pairs of particles are annihilated and a particle is created with probability $\mathcal{N}_p/z$ if the number of neighboring pairs $\mathcal{N}_p \geqslant 1$. In model D we consider that the creation can occur only if $\mathcal{N}_p \geqslant 2$ (Fig. 2).

For any of the above model versions, a phase transition is expected to separate an active regime (stable for low α) from an absorbing phase (stable for larger α) at a threshold value $\alpha = \tilde{\alpha}$. Actually, as we are going to see that three models present infinitely many absorbing states. Such a fact makes standard approaches, such as spreading experiments, difficult to use since the dynamic exponents present values dependent on the initial condition [19–22]. Thus, in order to analyze the transition by means of distinct (and unambiguous) procedures, we first study the order-parameter ϕ decays starting from a fully occupied initial condition for distinct

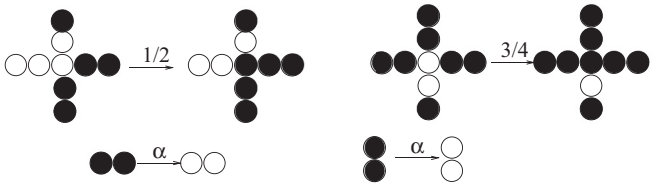

FIG. 2. Examples of transition rates for model D. Note that there is no particle creation if the number of pairs of particles $\mathcal{N}_p$ is smaller than 2.

independent runs. In the case of continuous transitions, ϕ decays algebraically as $\phi \sim t^{-\theta}$ at the critical point, with θ the associated critical exponent. Conversely, at a discontinuous transition ϕ is not expected to present a power law decay. This crucial difference is an important indication of the phase transition type. To further confirm the results, we plot the probability distribution P_ϕ (in the steady regime) assuming different initial configurations. A bimodal distribution points to a phase coexistence, whereas a single-peaked distribution, with its position continuously moving by changing α, corresponds to a continuous transition.

III. NUMERICAL RESULTS

Numerical simulations will be performed in square lattices of size L^2 and periodic boundary conditions. For the time decay analysis, we consider $L = 200$, whereas the probability distributions have been evaluated for L ranging from 40 to 120. Since isolated particles cannot create new ones, for this latter study, some extra conditions are required. Following Ref. [15], the extremities of the lattice are fully occupied by particles that cannot be removed. Thus, at any moment, there are at least four empty active sites that allow for the creation of particles. In addition, since in three of four models isolated particles cannot create new offsprings or be removed, whenever the system reaches the absorbing state a randomly chosen site and its nearest-neighbor sites are fulfilled by particles. In the first analysis, we show in Fig. 3 the main results for model

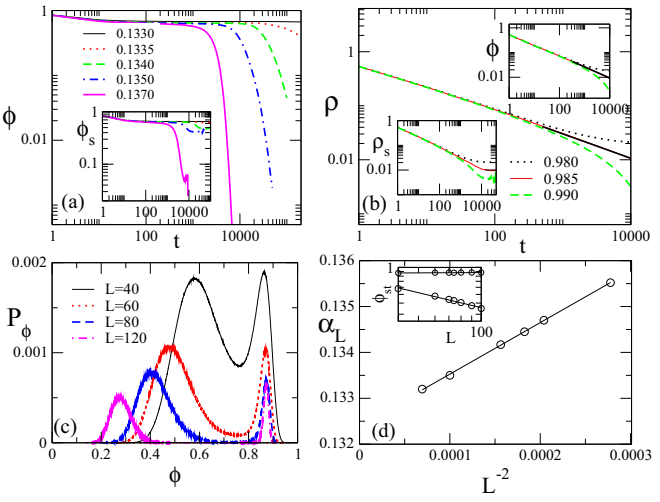

FIG. 3. (Color online) For model A and distinct α's, we plot in (a) the time decay of the order parameter ϕ evaluated over all and over only survived (inset) runs, respectively. In order to compare, we plot in (b) the time decay of the order parameter ρ for distinct α's by considering the $\mathcal{N} \geqslant 1$ creation with pair annihilation [23]. The black line in the middle curve has slope $\theta = 0.4505(10)$. The upper inset in (b) shows the time decay of ϕ (fraction of particles surrounded by at least $\mathcal{N} = 1$ occupied sites) over all runs and the lower inset shows the time decay of ρ measured over only survived runs. In (c) we plot the probability distribution P_ϕ for distinct L's at α_L, in which the peaks present the same height. The scaling plot of α_L vs L^{-2} is shown in (d). In the inset, we show a log-log plot of steady order parameters ϕ_{st}, in the active ϕ_{ac} and absorbing ϕ_{ab} phases, vs L.

A. In order to compare, we also show results for the particle creation in the presence of $\mathcal{N} \geqslant 1$, as studied by Dickman and Dickman [23]. One difference between the $\mathcal{N} \geqslant 1$ and $\mathcal{N} \geqslant 2$ cases [shown in Figs. 3(b) and 3(a), respectively] is that in the latter case any configuration devoid of pairs is absorbing and thus the system presents infinitely many absorbing states. Unlike the $\mathcal{N} \geqslant 1$ case, the phase transition is not ruled by the particle density ρ for $\mathcal{N} \geqslant 2$, but for the fraction ϕ of active particles (e.g., occupied sites presenting at least $\mathcal{N} = 2$ occupied neighbors). Another difference concerns the time decay behaviors. For $\mathcal{N} \geqslant 1$ [Fig. 3(b)], all curves decay algebraically for low t, deviating from such behavior off the critical point for larger t. For $\alpha_c \sim 0.985$ the power law is present for sufficient large times, with an exponent consistent with the DP value $\theta = 0.4505(10)$ [1]. Such an estimate for α_c agrees very well with the value 0.9846(1) obtained by Dickman and Dickman [23]. A similar exponent is obtained for the fraction ϕ of occupied sites presenting at least $\mathcal{N} = 1$ occupied neighbor. In contrast, for $\mathcal{N} \geqslant 2$ [Fig. 3(a)] the behavior of ϕ changes abruptly from a threshold value $\tilde{\alpha} \sim 0.1330$. For $\alpha < \tilde{\alpha}$ the activity survives indefinitely, dying off exponentially for $\alpha > \tilde{\alpha}$. Averages calculated only from survival runs enhance the above differences. Whenever in the nonrestrictive case ρ_s decays algebraically toward a constant value, the restriction also provokes distinct regimes. For $\alpha < \tilde{\alpha}$, ϕ_s saturates in a value close to ϕ (indicating the survival of almost all runs), whereas for $\alpha > \tilde{\alpha}$ it decays exponentially, reaching a lower saturated value. The existence of a discontinuous transition for $\mathcal{N} \geqslant 2$ is confirmed by plotting P_ϕ for distinct system sizes, as shown in Fig. 3(c). For all L's, it presents a bimodal shape, with well defined peaks signaling active ϕ_{ac} and absorbing ϕ_{ab} phases. The former changes very mildly with L, reaching the value $\sim$0.877, whereas the latter vanishes following the scaling relation $L^{-0.63(5)}$. In addition, the difference between α_L and α_0, in which the bimodal probability distribution has peaks of equal height for finite L and $L \to \infty$, respectively, scales with L^{-2}. Using this asymptotic scale relation, we obtain the extrapolated value $\alpha_0 = 0.1326(2)$, which agrees very well with the previous estimate. We note that such a dependence on L is similar to equilibrium discontinuous transitions [24,25].

Next we consider model B [exemplified by interaction rules (a)–(c) in Fig. 1], whose results are summarized in Fig. 4. As in model A, such a version presents infinitely many absorbing states and the decay of the order parameter also presents two distinct regimes from a threshold value $\tilde{\alpha} \sim 0.1310$. For $\alpha < \tilde{\alpha}$, it converges to a well defined value, indicating indefinite activity, whereas the exponential decay for $\alpha > \tilde{\alpha}$ signals full activity extinction. The pseudotransition points α_L, in which the two peaks of the probability distribution have the same height, also scale with L^{-2} for $\mathcal{N} \geqslant 2$, from which we get the extrapolated estimate $\alpha_0 = 0.1309(1)$. Such a value agrees very well with the previous estimate $\tilde{\alpha} \sim 0.1310$ [Fig. 4(b)]. The dependences on L of the steady order parameters ϕ_{ac} and ϕ_{ab} are also similar to those obtained for the previous model. Whenever ϕ_{ac} also changes very mildly with L, converging to the value $\sim$0.785, ϕ_{ac} vanishes following the scaling relation $\phi_{ab} \sim L^{-0.55(8)}$, which is similar to the pair annihilation case. As a result of three-particle annihilation, the compact cluster is somewhat less compact than the value for model A. Despite the Elgart-Kamenev conjecture that predicts a continuous

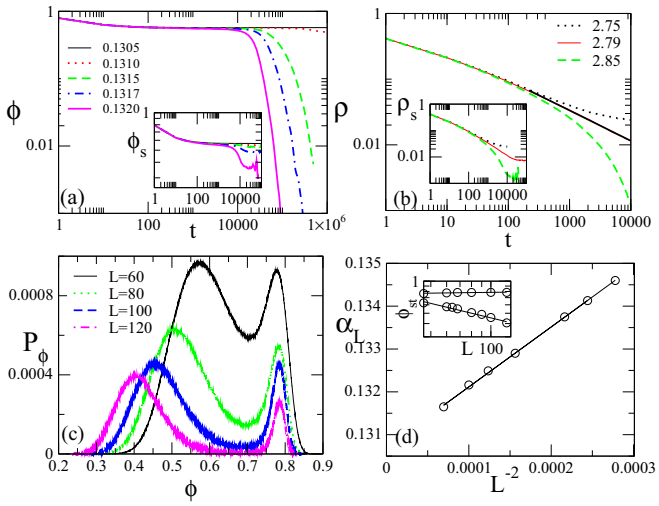

FIG. 4. (Color online) For model B and distinct α's, we plot in (a) the time decay of the order parameter ϕ evaluated over all and over only survived (inset) runs, respectively. In order to compare, we plot in (b) the time decay of the order parameter ρ for distinct α's by considering the $\mathcal{N} \geqslant 1$ creation case with triplet annihilation. The black line in the middle curve has slope $\theta = 0.4505(10)$. The inset in (b) shows the time decay of ρ measured over only survived runs. In (c) we plot the probability distribution P_ϕ for distinct L's at α_L, in which the peaks present the same height. The scaling plot of α_L vs L^{-2} is shown in (d). In the inset, we show a log-log plot of steady order parameters ϕ_{st}, in the active ϕ_{ac} and absorbing ϕ_{ab} phases, vs L.

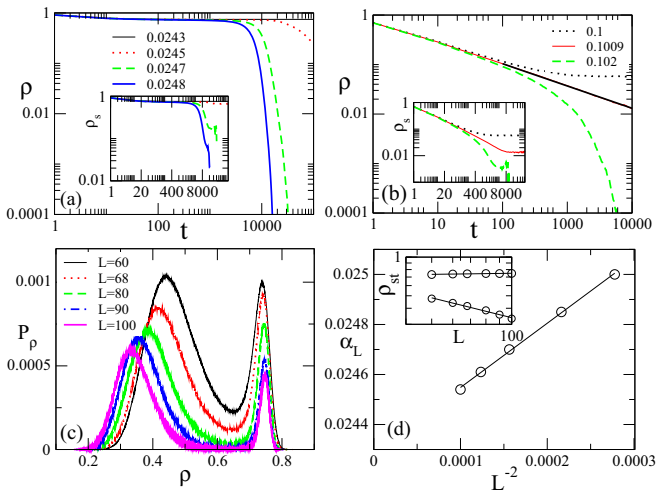

FIG. 5. (Color online) For model C and distinct α's, we plot in (a) the time decay of the order parameter ρ evaluated over all and over only survived (inset) runs, respectively. In order to compare, we plot in (b) the time decay of the order parameter ρ for distinct α's by considering the $\mathcal{N} \geqslant 1$ creation case, but with the same annihilation rule of model C. The black line in the middle curve has slope $\theta = 0.4505(10)$. The inset in (b) shows the time decay of ρ measured over only survived runs. In (c) we plot the probability distribution P_ρ for distinct L's at α_L, in which the peaks present the same height. The scaling plot of α_L vs L^{-2} is shown in (d). In the inset, we show a log-log plot of steady order parameters ρ_{st}, in the active ρ_{ac} and absorbing ρ_{ab} phases, vs L.

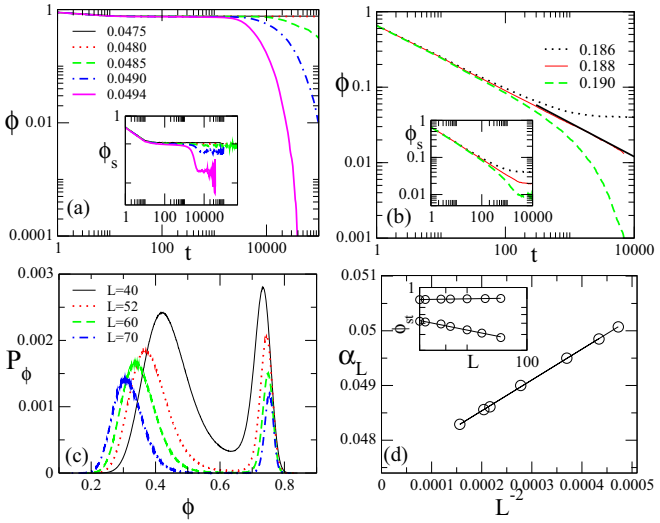

FIG. 6. (Color online) For the model D and distinct α's, we plot in (a) the time decay of the order parameter ϕ evaluated over all and over only survived (inset) runs, respectively. In order to compare, we plot in (b) the time decay of the order parameter ϕ for distinct α's for the original PCP. The black line in the middle curve has slope $\theta = 0.4505(10)$. The inset in (b) shows the time decay of ϕ measured over only survived runs. In (c) we plot the probability distribution P_ϕ for distinct L's at α_L, in which the peaks present the same height. The scaling plot of α_L vs L^{-2} is shown in (d). In the inset, we show a log-log plot of steady order parameters ϕ_{st}, in the active ϕ_{ac} and absorbing ϕ_{ab} phases, vs L.

transition (since $k = 3 > n = 2$), numerical results show that the phase transition is indeed first-order for $\mathcal{N} \geqslant 2$.

In order to strengthen the above conclusions, we examine model C, whose extinction includes all neighboring occupied sites of a given particle chosen at random. Unlike the previous examples, the system presents a single absorbing state and thus the dynamics is ruled by the particle density ρ. The results are summarized in Fig. 5. As in the previous examples, the creations in the presence of $\mathcal{N} \geqslant 1$ [Fig. 5(b)] and $\mathcal{N} \geqslant 2$ [Fig. 5(a)] behave very differently. Whenever in the former, ρ decays following a DP exponent $\theta = 0.4505(10)$ at $\alpha_c \sim 0.1009$; for $\mathcal{N} \geqslant 2$ one has two distinct regimes separated from a given threshold value $\tilde{\alpha} \sim 0.0244$. The probability distribution P_ρ [Fig. 6(c)] is also bimodal for $\mathcal{N} \geqslant 2$ and the positions of two equal peaks α_L also scale with L^{-2}, from which one gets the estimate $\alpha_0 = 0.0243(1)$, in excellent agreement with $\tilde{\alpha}$. The steady densities ρ_{st} also exhibit distinct dependences on the system size and are similar to previous cases. Whenever ρ_{ac} saturates in a constant value $\rho_{ac} \sim 0.747$ when L increases, ρ_{ab} vanishes according to the asymptotic law $L^{-0.52(5)}$.

Finally, we extend the restriction for the two-dimensional PCP (model D). By comparing Figs. 6(a) and 6(b), we see that similarly to previous models, the order parameter ϕ (the pair density in both cases) behaves differently from the original $\mathcal{N}_p \geqslant 1$ and $\mathcal{N}_p \geqslant 2$ versions. Whenever in the former ϕ decays with an exponent consistent with the DP value $\theta = 0.4505(10)$ at the phase transition (placed at $\alpha_c \sim 0.188$ [26]), a threshold value ($\tilde{\alpha} \sim 0.0480$) separates permanent extinction ($\alpha < \tilde{\alpha}$) from the full activity extinction ($\alpha > \tilde{\alpha}$) for $\mathcal{N}_p \geqslant 2$. Averages evaluated over survival runs corroborate the differences between both versions as well as the similarities among the above three examples. The probability distribution P_ϕ [Fig. 6(c)] also presents two peaks for $\mathcal{N}_p \geqslant 2$, whose α_L's scale with L^{-2}, providing the extrapolated estimate $\alpha_0 = 0.0474(2)$, which is close to the above estimate. As in all previous restrictive examples, ϕ_{ac} and ϕ_{ab} also exhibit distinct dependences on the system size L. Whenever ϕ_{ac} reaches the constant value $\sim$0.755 in the thermodynamic limit, ϕ_{ab} vanishes according to the relation $L^{-0.63(5)}$, which is consistent with all previous examples.

IV. CONCLUSION

We presented strong evidence of a minimal mechanism leading to a first-order transition into absorbing states for short-range systems. In all cases, results differing greatly from their original cases (in which the phase transitions are unambiguously continuous) have been achieved. The onset of a threshold value separating endless activity from an exponential decay toward the full extinction as well as bimodal distributions with (pseudo) transition points scaling on the system volume strongly suggests that the particle creation in the presence of a minimal neighborhood (for all studied models it is 2) constitutes a robust and fundamental ingredient determining the phase coexistence in short-range contact processes. An understanding about the role of such a particle creation requirement is achieved by performing mean-field calculations. By taking the correlation at the level of two sites, in all cases low-density states become unstable (with α increasing with ρ), signaling a jump. In contrast, for the nonrestrictive versions, ρ always decreases with α. As a final remark we note that the study of other restrictive processes, including the diffusion of particles and competitive dynamics, should be addressed in future work.

ACKNOWLEDGMENTS

I acknowledge Gandhi Viswanathan, M. W. Beims, and M. G. E. da Luz for critical readings of this manuscript and the research grant from CNPQ 307431.

[1] J. Marro and R. Dickman, *Nonequilibrium Phase Transitions in Lattice Models* (Cambridge University Press, Cambridge, 1999).
[2] G. Odor, Rev. Mod. Phys. **76**, 663 (2004).
[3] K. A. Takeuchi, M. Kuroda, H. Chaté, and M. Sano, Phys. Rev. Lett. **99**, 234503 (2007).
[4] T. E. Harris, Ann. Probab. **2**, 969 (1974).
[5] F. Schlögl, Z. Phys. **253**, 147 (1972).

[6] R. M. Ziff, E. Gulari, and Y. Barshad, Phys. Rev. Lett. **56**, 2553 (1986).
[7] See, for example, S. Lubeck, J. Stat. Phys. **123**, 193 (2006).
[8] A. L. Toom, in *Multicomponent Random Systems*, edited by R. L. Dobrushin and Ya. G. Sinai, Advances in Probability Vol. 6 (Dekker, New York, 1980), pp. 549–575.
[9] H. K. Janssen, Z. Phys. B **42**, 151 (1981); P. Grassberger, *ibid*. **47**, 365 (1982).
[10] V. Elgart and A. Kamenev, Phys. Rev. E **74**, 041101 (2006).
[11] H. Hinrichsen, arXiv:cond-mat/0006212.
[12] S.-C. Park, Phys. Rev. E **80**, 061103 (2009).
[13] D.-J. Liu, X. Guo, and J. W. Evans, Phys. Rev. Lett. **98**, 050601 (2007); X. Guo, D.-J. Liu, and J. W. Evans, J. Chem. Phys. **130**, 074106 (2009).
[14] C. J. Wang, D. J. Liu, and J. W. Evans, Phys. Rev. E **85**, 041109 (2012).
[15] E. F. da Silva and M. J. de Oliveira, J. Phys. A **44**, 135002 (2011); Comput. Phys. Commun. **183**, 2001 (2012).
[16] C. Varghese and R. Durrett, Phys. Rev. E **87**, 062819 (2013).
[17] I. Jensen, Phys. Rev. Lett. **70**, 1465 (1993).
[18] J. K. L. da Silva and R. Dickman, Phys. Rev. E **60**, 5126 (1999).
[19] I. Jensen and R. Dickman, Phys. Rev. E **48**, 1710 (1993).
[20] M. A. Muñoz, G. Grinstein, R. Dickman, and R. Livi, Phys. Rev. Lett. **76**, 451 (1996).
[21] M. A. Muñoz, G. Grinstein, R. Dickman, and R. Livi, Physica D **103**, 485 (1997).
[22] M. A. Muñoz, G. Grinstein, and R. Dickman, J. Stat. Phys. **91**, 541 (1998).
[23] A. G. Dickman and R. Dickman, J. Stat. Mech. (2010) P05009.
[24] C. Borgs and R. Kotecký, J. Stat. Phys. **61**, 79 (1990); Phys. Rev. Lett. **68**, 1734 (1992).
[25] C. E. Fiore and M. G. E. da Luz, Phys. Rev. Lett. **107**, 230601 (2011).
[26] In fact, our estimate is different from the estimate $\alpha_c = 0.200\,51(1)$ [18] as a result of a slightly different dynamics implementation.